

1
2
3
4
5
6
7
8
9
10
11
12
13
14
15
16
17
18
19
20
21
22
23
24
25
26
27

A Normative Database of A-Scan Data Using the Heidelberg Spectralis Spectral Domain
Optical Coherence Tomography Machine

Joos Meyer^{1*¶}; Roshan Karri^{2¶}; Helen Danesh-Meyer^{3&}; Kate Drummond^{4&}; Andrew
Symons^{2&}

¹Ophthalmology Department, The Royal Melbourne Hospital, 300 Grattan St, Parkville, VIC
3050, Australia

²The Faculty of Medicine, Dentistry and Health Sciences, The University of Melbourne,
Parkville, VIC 3010, Australia

³Faculty of Medical and Health Sciences, The University of Auckland, 85 Park Rd, Grafton,
Auckland 1023, New Zealand

⁴The Department of Neurosurgery, The Royal Melbourne Hospital, 300 Grattan St, Parkville,
VIC 3050, Australia

*Corresponding author:
Email: joos.meyer@mh.org.au

¶These authors contributed equally to this work.
&These authors also contributed equally to this work.

28 **Abstract**

29 **Purpose**

30 Develop the first normative database of macular and circumpapillary scans with
31 reference values at the level of the A-scan using the Heidelberg Spectralis Optical Coherence
32 Tomography (OCT) machine.

34 **Methods**

35 This study is a retrospective cross sectional analysis of macular and circumpapillary OCT
36 scans of healthy individuals. All participants had a full ophthalmic examination, including
37 best corrected visual acuity, intraocular pressure, biomicroscopy, posterior segment
38 examination and OCT scan. The volume and thickness of each of the nine Early Treatment
39 Diabetic Retinopathy zones at the macula were analysed for the total retinal thickness, retinal
40 nerve fibre layer (RNFL), ganglion cell layer (GCL) and inner plexiform layer (IPL). The
41 thickness of the circumpapillary RNFL was analysed at the disc. De-identified A-scans were
42 extracted from the OCT machine as separate tab-separated text file and made available
43 according to the data sharing statement.

44 **Results**

45 Two-hundred eyes from 144 participants were included of which 98 (49%) were female. The
46 mean age (SD) was 48.52 (17.52). Participants were evenly distributed across four age
47 groups and represented nine broad ethnic groups in proportions comparable to the local
48 distribution. All the macular scans were 20° x 20° (5.9 mm x 5.9 mm), with a total scan
49 density between 12,800 and 49,152 A-scans. The peripapillary scans were all 12° (3.5 mm),
50 at a scan density of 768 A-scans. The mean retinal, GCL and IPL volumes were significantly
51 greater in males than females. Age and total retinal volume ($r = -0.2561$), GCL volume ($-$
52 0.2911) and IPL volume (-0.3194) were negatively correlated. No significant correlation was
53 found between the RNFL and age.

54 **Conclusion**

55 This study provides a normative database of macular and circumpapillary scans with
56 reference values at the level of the A-scan using the Heidelberg Spectralis Optical Coherence
57 Tomography (OCT) machine.

58 Introduction

59 Optical coherence tomography (OCT) is a non-invasive imaging technology that uses low
60 coherence interferometry to create two-dimensional cross-sectional imaging of biological
61 systems.[1] In ophthalmic practice, OCT is used to image and measure the retinal architecture
62 and changes that occur in disease states. Diseases, such as glaucoma and compressive optic
63 neuropathy, manifest distinct changes on OCT scans, particularly on the inner retinal layers.
64 Important OCT measurements for both diseases include the circumpapillary retinal nerve
65 fibre layer (RNFL), macular RNFL and the macular ganglion cell layer (GCL).[2,3]

66 The Early Treatment Diabetic Retinopathy Study (ETDRS) grid is a standardised pattern of
67 dividing and measuring the thickness and volume profile of the retina.[4] It was first
68 introduced in 1980, and is still the primary method of reporting.[5] Since its inception,
69 additional grid patterns have been developed; however, there is limited flexibility for
70 clinicians and researchers to explore novel patterns of segmentation within any currently
71 commercially available software.

72 For the macular, the standard 20° x 20° scan consists of horizontally stacked scan lines to
73 create a square scan area. Each horizontal line is termed a B-scan, and each of these
74 comprises a row of equally distanced A-scans. The A-scan represents the most basic unit of
75 interrogation from which the rest of the scan is generated. The scan density of the Heidelberg
76 Stratus (Heidelberg Engineering, Heidelberg, Germany) varies between 25,000 and 50,000
77 A-scans. For the optic disc, the standard circumpapillary scan consists of a 360° radial scan
78 of 720 A-scans. Extracting the A-scan data enables the exploration of OCT changes that do
79 not conform to the spatial distribution of the predefined grid patterns.

80 A normative database of scans is needed for comparison to validate changes in disease states.
81 To the author's knowledge, a normative database that contains both macular and
82 circumpapillary scans, which includes reference values for each A-scan of the Heidelberg
83 Stratus, does not currently exist.

84 The purpose of this study is to report the normative values for macular and optic disc scans
85 within the standard ETDRS grid and at the level of the A-scan. This study aims to help
86 clinicians and researchers to identify patterns of change that occur outside the standard
87 segmentation patterns of the retina.

88 Methods

89 Study Population

90 This study is a retrospective cross-sectional analysis of 200 normal eyes that had a visual
91 assessment and an OCT scan. The participants included patients of The Royal Melbourne
92 Hospital (RMH) who were found to have no ocular pathology or systemic disease that could
93 manifest in retinal changes. The RMH database was used to create this normative database.

94 Approximately 50,000 eyes have been scanned since 2012 on the Heidelberg Spectralis
95 machine at The RMH. The database was queried for normal OCT scans, and the potential
96 participant's medical records were checked against inclusion and exclusion criteria. All of the
97 participants had a full ophthalmic examination, including their Snellen best corrected visual
98 acuity (BCVA), intraocular pressure (IOP), biomicroscopy, posterior segment examination
99 and OCT scan. The participant's medical records were examined for any exclusions.

100 The retrospective inclusion criteria included healthy participants, aged 18 to 88, with a
101 BCVA of 6/12 (20/40) on the Snellen chart measured at 6 m (20 feet), and high quality
102 macular and peripapillary OCT scans (signal strength >15dB). The exclusion criteria
103 included a history of any: (i) anterior segment disease (except cataracts); (ii) retinal disease;
104 (iii) glaucoma; (iv) uveitis; (v) optic nerve disease; (vi) systemic disease known to affect the
105 retina (e.g., diabetes); (vii) neurological disease; (viii) pituitary disease; (ix) intracranial
106 space-occupying lesions; (x) previous neurosurgery; (xi) retinal lasers; (xii) vitrectomy; (xiii)
107 topical or systemic anti-vascular endothelial growth factor treatment; (xiv) IOP lowering
108 medications; (xv) chemotherapy; or (xvi) previous systemic or active topical steroid use. The
109 excluding biomarkers included peripapillary atrophy, RNFL haemorrhage, optic disc
110 notching or thinning, age-related macular degeneration (including drusen) or macular disease
111 on OCT scans. Ethnicity data were collected from the participants and categorised according
112 to the Australian Bureau of Statistics' (ABS) Australian Standard Classification of Cultural
113 and Ethnic Groups (ASCCEG).[6]

114 This study was approved by the Human Research and Ethics Committee of The RMH. It was
115 conducted according to the Declaration of Helsinki in its currently applicable version.

116 **Optical Coherence Tomography**

117 All the OCT scans were performed with the Heidelberg Spectralis Spectral Domain (SD)
118 OCT and the Heidelberg Eye Explorer version 6.7.13.0 (Heidelberg Engineering, Heidelberg,
119 Germany). All scans were completed by experienced medical imaging personnel at The RMH
120 medical imaging department; they were performed in a dark room as per the standard hospital
121 protocol. Only the well-centred scans (>15dB quality) were included in the analysis. The
122 number of dioptres focus spherical was recorded for each scan as a proxy for the refractive
123 error. The scans were quality controlled for the accurate segmentation of each macular retinal
124 inner layer and peripapillary scan, and an experienced grader manually corrected any
125 aberrations.

126 The macular scans were divided into 1 mm, 3 mm and 6 mm rings on the macular ETDRS
127 map. The inner ring was defined as the central thickness, and the middle and outer rings were
128 divided into four zones designated as the superior, nasal, inferior and temporal zones. The
129 average thickness in each of the nine zones, the macular thickness and the full 360°
130 peripapillary scans were included in the final analysis.

131 **A-Scan Data**

132 The A-scans were extracted from the machine using the Heidelberg Spectralis Layer
133 Segmentation Export Special Function version 6.0. Each file contained the results from the
134 automatic retinal layer segmentation algorithm of a Spectralis OCT machine as a
135 tab-separated text file. The distance values of each A-scan location were represented as
136 relative coordinates in nanometres from the probe to the layer segmentation interface. The
137 normative values of the A-scans were compiled as a de-identified single data array per patient,
138 per eye.

139 **Statistical Analysis**

140 All analyses were conducted in the R statistical programming language using RStudio
141 version 1.3.1073 (Boston, USA).[7] The exploratory data analysis and data visualisation were
142 performed using the ggplot2 package.[8] The descriptive statistics were reported as the mean,
143 standard deviation and the first, fifth and 95th percentiles. An independent t-test was used to
144 compare the thickness values between groups. The correlation between measurements was
145 found using Pearson correlation coefficients. A multivariate analysis was used to consider the
146 effects of age and gender; an alpha of 0.05 was considered significant. The chi-square
147 goodness of fit test was used to compare the observed distribution of ABS ethnicities to the
148 expected distribution in Melbourne, Australia.

149 **Results**

150 **Study participants**

151 Two-hundred eyes from 146 participants were included in the final analysis. There were 69
152 (47%) females and 77 (53%) males, and the mean age (SD) was 48.52 (17.52) (range: 21–85).
153 Mean (SD) scan focus was 0.29 D (1.96) (range: -6.48–7.86). The participants were evenly
154 distributed across the age groups (Table 1). Females were slightly under-represented in the
155 younger age groups and over-represented in the older age groups. This study included 101
156 (50.5%) right eyes and 99 (49.5%) left eyes. Participants from nine broad ethnicity groups
157 were included in the study (Table 2). There were significant differences in the proportion of
158 broad ethnic categories compared to the census population proportions in four out of the nine
159 groups.

160 **Table 1. Distribution of participants by age group and gender**

Age group	Participants, n (%)	Eyes, n (%)	Females, n (%)
18–33	37 (25.3)	52 (26.0)	14 (37.8)
34–50	41 (28.0)	62 (31.0)	13 (31.7)
51–68	43 (29.5)	57 (28.5)	27 (62.8)
69–88	25 (17.1)	29 (14.5)	15 (60.0)

161 **Table 2. Australian Bureau of Statistics Australian Standard Classification of Cultural**
162 **and Ethnic Groups broad group classification of participants**

Broad ethnicity category	Participants, Melbourne	P
--------------------------	-------------------------	---

	n (%)	(%)	
North African and Middle Eastern	15 (7.5)	1.9	<0.001
Northeast Asian	4 (2)	5.1	0.0644
Northwest European	9 (4.5)	5.3	0.7283
Oceanian	111 (55.5)	68.5	<0.001
People of the Americas	2 (1)	0.8	1
Southeast Asian	14 (7)	6.0	0.644
Southern and Central Asian	22 (11)	6.9	0.031
Southern and Eastern European	15 (7.5)	4.5	0.0666
Sub Saharan African	8 (4)	1.0	<0.001

163 **A-scans**

164 Two-hundred de-identified tab separated text files were exported from the Heidelberg Stratus
165 SD OCT machine. All the macular scans were 20° x 20° (5.9 mm x 5.9 mm), with 25 to 96
166 B-scans, and 512 A-scans per B-scan with the automatic real-time mode active. The total
167 scan density was between 12,800 and 49,152 A-scans. The peripapillary scans were all 12°
168 (3.5 mm diameter), at a scan density of 768 A-scans. All the scan data are available,
169 according to the data sharing statement.

170 **Distribution of macular and circumpapillary measurements**

171 The mean (SD) total retinal volume was 8.67 mm³ (0.38) (range: 7.65–9.58). The
172 macular RNFL volume (SD) was 0.96 mm³ (0.11) (range: 0.72–1.26). The GCL volume (SD)
173 was mm³ 1.09 (0.10) (range: 0.82–1.31) and the inner plexiform layer (IPL) volume (SD)
174 was 0.89 mm³ (0.07) (range: 0.7–1.05). See Figs 1 and 2 demonstrating layer measurement
175 distributions.

176

177 **Fig 1. Histogram and fitted normal distribution curves of macular optical coherence**
178 **tomography measurements.** (A) Total retinal volume. (B) Retinal nerve fibre layer volume.
179 (C) Ganglion cell layer volume. (D) Inner plexiform layer volume.

180

181 **Fig 2. Histogram and fitted normal distribution curve of mean peripapillary retinal**
182 **nerve fibre layer thickness values**

183 **Difference in measurements between males and females**

184 The multivariate regression analysis controlling for age and ethnicity (Table 3) showed that
185 the retinal and GCL volumes were significantly less for females. The total RT was
186 significantly lower in females in all sectors except for the superior outer sector. The same
187 was true for the central, nasal inner, temporal inner, inferior inner macular RNFL, GCL and
188 IPL thicknesses. The GCL and IPL also showed that females had significantly lower superior
189 inner sectors. There were no significant differences found at the peripapillary RNFL between
190 males and females (Table 4).

191 **Table 3. Female regression coefficient in multivariate analysis controlling for age with**
 192 **macular sectorial thickness values as outcome**

Sector	Retina	p	mRNFL	p	GCL	p	IPL	p
Volume	-0.175751	***	-0.0112461		-0.0309332	*	-0.0121464	
Centre	-14.58119	***	-1.287385	***	-2.741456	***	-2.84705	***
Nasal inner	-11.15093	***	-0.86165	*	-2.44177	**	-1.23396	*
Nasal outer	-5.82186	**	-0.602074		-0.34252		0.09550	
Superior inner	-10.07472	***	-0.92011		-1.82976	**	-1.00703	*
Superior outer	-2.88614		0.97539		-0.51977		0.02971	
Temporal inner	-10.548601	***	-0.503470	*	-3.26108	***	-1.68946	**
Temporal outer	-4.83874	*	-0.39463		-1.01023		-0.97755	
Inferior inner	-10.35359	***	-1.438830	**	-1.97374	**	-1.07487	*
Inferior outer	-4.99137	*	-0.33538		-0.37526		-0.13309	

193 P-values are coded as: ***<0.001, **<0.01 and *<0.05.

194 **Table 4. Female regression coefficient in multivariate analysis controlling for age with**
 195 **peripapillary retinal nerve fibre layer sectorial thickness values as outcome**

Sector	Disc	p
Total	-0.58076	
Nasal superior	2.71149	
Nasal	-0.18586	
Nasal inferior	-0.08341	
Temporal superior	-2.02026	
Temporal	-0.84995	
Temporal inferior	-2.00331	

196 P-values are coded as: ***<0.001, **<0.01 and *<0.05.

197 **Decrease in thickness per decade**

198 The mean retinal, GCL and IPL volumes were found to be significantly greater in males than
 199 females (Table 5). The mean volumes, ETDRS segment thickness values and the first, fifth
 200 and 95th percentile values were grouped by age for each macular layer (Table 6-9). The mean
 201 (SD) peripapillary RNFL thickness was 99.7 μ m (9.47) (range: 78–137). The mean
 202 peripapillary RNFL thicknesses were grouped by age (Table 10).

203 **Table 5. Mean volumes by gender**

Volume	Male	Female	P
Retinal	8.77 (0.401)	8.56 (0.326)	>0.0001
RNFL	0.961 (0.122)	0.957 (0.101)	0.7943
GCL	1.11 (0.11)	1.07 (0.0764)	0.002346
IPL	0.903 (0.0801)	0.879 (0.0622)	0.01882
Disc RNFL thickness	99.9 (9.66)	99.6 (9.31)	0.8

204 **Table 6. Macular retinal thickness distribution by age group, showing mean, first, fifth and 95th percentile values for each segment**

Retina	18–33				34–50				51–68				69–88			
	Percentile				Percentile				Percentile				Percentile			
	x̄	1st	5th	95th												
Volume	8.74	7.99	8.11	9.13	8.76	7.77	8.22	9.27	8.59	8.12	8.16	9.45	8.48	7.66	7.71	9.02
Centre	270.56	228.5	239.3	306.8	280.50	228.6	246.1	308.0	279.05	220.7	237.0	320.2	270.17	233.0	240.0	305.4
Nasal inner	348.29	321.0	327.0	369.7	353.31	314.0	329.0	378.0	345.77	319.7	324.2	379.2	342.45	315.6	317.4	371.6
Nasal outer	321.37	294.6	298.1	341.9	319.76	280.4	298.1	338.0	312.86	283.0	293.6	343.6	308.34	278.6	280.0	333.6
Superior inner	343.29	254.7	320.1	368.3	351.45	310.1	334.1	375.0	342.33	312.0	320.4	369.2	339.69	308.6	311.2	365.8
Superior outer	302.37	272.0	276.7	321.8	301.40	269.5	285.0	320.0	296.14	273.7	278.8	322.6	291.38	259.1	262.8	310.6
Temporal inner	329.56	300.0	305.1	352.9	337.15	295.6	318.0	360.9	330.67	302.2	304.8	362.6	327.41	299.1	302.0	346.2
Temporal outer	286.73	257.5	267.1	300.5	286.18	251.7	263.1	304.0	282.26	263.0	265.8	315.0	278.62	244.1	247.8	299.2
Inferior inner	343.35	315.1	320.2	362.9	347.48	309.6	328.0	370.9	339.61	316.0	316.8	371.0	338.31	309.4	314.2	361.2
Inferior outer	292.69	258.1	266.1	309.4	291.69	266.8	272.0	308.0	286.37	264.1	268.4	314.2	282.48	253.3	255.6	303.2

205 **Table 7. Macular retinal nerve fibre layer thickness distribution by age group, showing mean, first, fifth and 95th percentile values for**
206 **each segment**

RNFL	18–33				34–50				51–68				69–88			
	Percentile				Percentile				Percentile				Percentile			
	x̄	1st	5th	95th												
Volume	0.95	0.77	0.81	1.12	0.96	0.74	0.76	1.16	0.94	0.75	0.78	1.11	1.01	0.79	0.88	1.16
Centre	12.42	8.0	9.0	16.0	12.98	6.6	10.0	16.0	12.91	8.6	9.0	16.2	12.41	8.0	8.8	15.0
Nasal inner	22.06	17.5	19.0	26.0	22.31	17.0	18.0	27.0	21.96	17.0	18.0	27.0	22.69	18.0	18.4	28.0
Nasal outer	51.73	39.0	43.0	65.0	51.44	38.0	38.0	69.9	48.79	29.1	38.8	58.8	53.24	25.5	40.6	64.0
Superior inner	25.54	19.5	21.6	31.4	26.02	19.6	20.1	32.0	25.28	19.6	20.8	31.2	27.45	20.8	23.0	35.2
Superior outer	38.15	27.5	31.1	45.0	39.26	28.6	30.1	50.8	37.68	26.0	28.6	45.6	41.62	30.4	34.4	50.8
Temporal inner	17.56	15.0	16.0	19.0	17.90	16.0	16.0	20.0	18.37	16.0	16.0	21.2	18.38	16.3	17.0	20.6
Temporal outer	18.73	16.0	17.0	20.0	18.77	16.6	17.0	21.0	20.39	16.6	17.0	23.0	21.07	19.0	19.0	23.0
Inferior inner	26.37	22.0	23.0	31.0	26.53	19.0	21.1	34.0	26.42	20.1	22.0	31.6	27.00	22.3	23.0	32.6

Inferior outer	42.27	30.0	32.0	49.0	41.50	30.2	32.0	53.0	41.79	30.0	31.8	53.2	42.72	33.0	33.4	51.2
----------------	-------	------	------	------	-------	------	------	------	-------	------	------	------	-------	------	------	------

207 **Table 8. Macular ganglion cell layer thickness distribution by age group, showing mean, first, fifth and 95th percentile values for each**
 208 **segment**

GCL	18–33				34–50				51–68				69–88			
	Percentile				Percentile				Percentile				Percentile			
	x□	1st	5th	95th												
Volume	1.10	0.88	0.95	1.23	1.12	0.89	0.99	1.25	1.06	0.89	0.93	1.22	1.04	0.84	0.90	1.13
Centre	16.00	9.5	10.0	24.5	16.55	7.2	10.1	23.0	15.33	8.0	8.0	21.2	14.45	8.3	9.0	22.0
Nasal inner	54.10	39.1	46.7	59.9	54.69	41.2	46.0	62.0	51.32	37.5	45.0	58.2	51.79	39.4	43.4	58.0
Nasal outer	38.77	31.5	34.0	43.0	38.65	31.2	32.1	44.0	37.26	30.1	31.8	43.0	35.52	29.3	30.0	40.0
Superior inner	53.96	41.1	48.0	60.5	55.08	43.2	48.1	63.0	51.49	40.1	44.0	59.0	51.79	40.7	45.0	57.0
Superior outer	35.13	28.0	30.0	41.0	35.06	28.6	29.1	39.0	33.95	29.0	29.0	40.2	32.45	27.6	29.0	36.0
Temporal inner	47.94	30.5	38.7	56.5	50.63	38.0	40.1	58.0	46.68	34.7	39.2	54.0	47.03	33.0	38.4	54.6
Temporal outer	36.85	25.5	30.6	44.0	37.35	29.6	30.1	44.9	34.30	28.0	29.0	40.4	34.62	27.3	28.0	40.2
Inferior inner	53.60	42.1	47.6	60.0	54.21	43.4	47.0	63.0	50.96	42.2	44.0	58.4	51.55	40.2	46.0	57.2
Inferior outer	33.83	28.0	28.0	38.5	33.92	25.0	26.2	38.0	32.26	26.6	27.8	36.2	32.07	26.6	28.0	36.6

209 **Table 9. Macular inner plexiform layer thickness distribution by age group, showing mean, first, fifth and 95th percentile values for**
 210 **each segment**

IPL	18–33				34–50				51–68				69–88			
	Percentile				Percentile				Percentile				Percentile			
	x□	1st	5th	95th												
Volume	0.91	0.79	0.80	1.03	0.91	0.71	0.81	0.99	0.87	0.73	0.77	1.01	0.86	0.72	0.76	0.93
Centre	21.15	14.0	15.0	27.9	22.24	13.6	15.1	28.0	21.53	14.6	15.8	27.2	20.90	15.3	16.0	26.0
Nasal inner	44.12	34.5	39.0	50.0	44.35	35.6	38.1	50.0	42.21	35.1	37.0	48.0	42.07	33.4	37.4	46.0
Nasal outer	29.75	24.5	25.6	34.0	29.31	22.0	24.1	33.0	28.21	22.6	23.8	33.0	26.90	22.0	22.4	30.6
Superior inner	42.58	34.5	37.1	47.0	42.82	35.8	38.0	49.0	40.25	33.1	34.8	46.2	40.24	34.0	34.8	43.6
Superior outer	28.87	23.5	25.0	33.0	28.10	21.6	24.0	32.0	27.28	23.0	23.8	33.0	26.38	22.3	23.4	29.6
Temporal inner	42.17	30.6	35.6	48.5	43.16	34.6	38.0	49.0	41.16	33.7	35.8	47.2	41.07	32.1	35.8	45.0

Temporal outer	32.52	26.5	27.6	36.5	32.44	24.2	27.0	37.0	30.77	25.0	26.8	36.2	30.79	26.3	27.0	34.6
Inferior inner	42.46	35.0	38.0	47.5	42.35	34.6	37.0	47.0	40.00	34.1	35.8	45.0	40.69	34.6	36.0	44.6
Inferior outer	27.44	22.0	23.0	32.0	27.29	20.0	20.2	31.0	25.91	20.6	22.0	30.0	26.10	22.3	23.0	29.6

211

212 **Table 10. Retinal nerve fibre layer disc distribution by age group, showing mean, first, fifth and 95th percentile values for each segment**

Disc	18–33				34–50				51–68				69–88			
	Percentile				Percentile				Percentile				Percentile			
	x̄	1st	5th	95th	x̄	1st	5th	95th	x̄	1st	5th	95th	x̄	1st	5th	95th
Total	99.96	82.5	86.1	113.5	101.34	83.6	87.0	120.8	98.42	82.0	83.8	112.0	98.55	79.7	84.8	109.2
Nasal superior	114.19	69.6	85.8	145.7	110.10	84.1	88.1	135.0	111.79	72.1	78.0	148.0	107.45	73.6	78.6	144.8
Nasal	74.90	48.5	50.6	103.3	78.39	50.8	57.0	99.9	76.02	53.7	56.8	95.0	79.79	58.1	63.4	100.8
Nasal inferior	111.96	61.5	71.2	149.8	115.85	70.0	79.0	152.7	112.68	75.6	81.4	157.2	112.48	77.5	84.8	153.0
Temporal superior	139.71	99.1	115.0	164.5	143.03	115.8	120.1	171.8	133.58	93.6	106.8	156.4	132.79	103.7	108.4	152.2
Temporal	71.37	51.5	54.7	92.1	69.37	57.2	58.0	84.0	68.89	52.8	57.0	83.2	70.14	46.2	57.0	90.2
Temporal inferior	141.50	91.0	119.6	166.9	145.55	117.1	120.1	183.7	139.56	89.3	111.2	173.4	135.28	115.3	116.4	149.2

213 Linear regression analysis showed a significant negative correlation between the total retinal
 214 volume and age ($r = -0.2561$), GCL volume and age (-0.2911) and IPL volume and age ($-$
 215 0.3194). There was no significant correlation found between the RNFL and age. Figs 3 and 4
 216 demonstrate trend lines for layer measurements against age. Table 11 demonstrates the
 217 regression analysis of segmental retinal thickness (RT) values against age. The strongest
 218 three significant negative associations were found in the superior inner IPL ($r = -0.3444$),
 219 nasal outer IPL ($r = -0.3217$) and inferior inner IPL ($r = -0.3179$) segments. The only
 220 significant positively correlated segment was the temporal inner RNFL ($r = 0.1929$). The only
 221 significant association between age and thickness at the peripapillary disc scan was the
 222 superior temporal sector ($r = -0.1910$) (Table 12).

223 **Fig 3. Scatter plot with trend line for macular optical coherence tomography**
 224 **measurements against age.** (A) Total retinal volume. (B) Retinal nerve fibre layer volume.
 225 (C) Ganglion cell layer volume. (D) Inner plexiform layer volume.

226 **Fig 4. Scatter plot with trend line for mean peripapillary retinal nerve fibre layer**
 227 **thickness against age**

228 **Table 11. Regression analysis of layer thickness (μm) against age (years) and p-value for**
 229 **each macular segment**

Segment	Retina		RNFL		GCL		IPL	
	R	p	R	p	R	p	R	p
Volume	-0.2561	0.0003	0.0658	0.3544	-0.2911	<0.0001	-0.3194	<0.0001
Centre	0.0089	0.9008	0.0011	0.9875	-0.1500	0.0340	-0.0585	0.4103
Nasal inner	-0.1821	0.0098	-0.0003	0.9969	-0.2821	0.0001	-0.2930	<0.0001
Nasal outer	-0.3151	<0.0001	-0.0574	0.4191	-0.3051	<0.0001	-0.3217	<0.0001
Superior inner	-0.1438	0.0421	0.0572	0.4214	-0.2954	<0.0001	-0.3444	<0.0001
Superior outer	-0.2466	0.0004	0.0964	0.1743	-0.2494	0.0004	-0.2873	<0.0001
Temporal inner	-0.1117	0.1152	0.1929	0.0062	-0.1847	0.0088	-0.2071	0.0033
Temporal outer	-0.1943	0.0058	<0.0001	0.3556	-0.2516	0.0003	-0.2001	0.0045
Inferior inner	-0.0532	0.4540	<0.0001	0.9996	-0.2841	<0.0001	-0.3179	<0.0001
Inferior outer	-0.2521	0.0003	0.0033	0.9627	-0.2233	0.0015	-0.2138	0.0024

230 **Table 12. Regression analysis of layer thickness (μm) against age (years) and p-value for**
 231 **each disc segment**

Segment	Disc	
	R	p
Total	-0.1050	0.139
Nasal superior	-0.1298	0.0671
Nasal	0.0654	0.3573
Nasal inferior	-0.0255	0.72
Temporal superior	-0.1910	0.0067
Temporal	-0.0533	0.4539
Temporal inferior	-0.1312	0.0642

233 **Association between refractive error and thickness**

234 Retinal thickness segments, except for the nasal outer, were not significantly
 235 correlated with refractive error. In order of magnitude, nasal outer ($r = -0.2020$), inferior
 236 outer ($r = -0.1570$) and inferior inner ($r = -0.1314$) RNFL segments were negatively
 237 correlated. Central RNFL was positively correlated ($r = 0.1426$). GCL segments were only
 238 negatively correlated; superior inner ($r = -0.2034$), nasal inner ($r = -0.1782$), temporal inner (r
 239 $= -0.1534$) and nasal outer ($r = -0.1478$). The IPL had the most segments significantly
 240 correlated with refractive error all of which were negative and included IPL volume ($r =$
 241 0.1668), nasal inner ($r = -0.2154$), nasal outer ($r = -0.1946$), superior inner ($r = -0.2205$),
 242 temporal inner ($r = -0.1755$), and inferior inner ($r = -0.2448$) (Table 13). Nasal ($r = 0.1863$)
 243 and nasal inferior ($r = 0.1924$) disc segments were significantly positively correlated while
 244 the temporal sector was negatively correlated ($r = -0.2365$).

245 **Table 13. Regression analysis of layer thickness (μm) against refractive error (dioptries)**
 246 **and p-value for each macular segment**

Segment	Retina		RNFL		GCL		IPL	
	R	p	R	p	R	p	R	p
Volume	-0.0877	0.2171	-0.1290	0.0687	-0.1138	0.1088	-0.1668	0.0182
Centre	0.0942	0.1847	0.1426	0.044	-0.0509	0.4744	0.0341	0.632
Nasal inner	-0.0475	0.5041	-0.0751	0.2905	-0.1782	0.0116	-0.2154	0.0022
Nasal outer	-0.1614	0.0225	-0.2020	0.0041	-0.1478	0.0374	-0.1946	0.0058
Superior inner	-0.0205	0.7733	-0.0769	0.2794	-0.2034	0.0039	-0.2205	0.0017
Superior outer	-0.0460	0.5178	-0.0228	0.7482	-0.0193	0.7857	-0.0822	0.2473
Temporal inner	-0.0339	0.6332	0.0723	0.3089	-0.1534	0.0301	-0.1755	0.0529
Temporal outer	-0.0413	0.5616	0.1210	0.2555	-0.0638	0.3695	-0.1073	0.1306
Inferior inner	-0.1129	0.1113	-0.1314	0.0637	-0.2102	0.3695	-0.2448	0.0005
Inferior outer	-0.1045	0.1407	-0.1570	0.0264	-0.0268	0.7065	-0.0390	0.5828

253

254 **Table 14. Regression analysis of layer thickness (μm) against refractive error (dioptries)**
 255 **and p-value for each disc segment**

Segment	Disc	
	R	p
Total	0.0899	0.2056
Nasal superior	0.0383	0.5903
Nasal	0.1863	0.0083
Nasal inferior	0.1924	0.0063
Temporal superior	-0.0722	0.3096
Temporal	-0.2365	0.0007
Temporal inferior	0.1029	0.1472

260

261 Discussion and Conclusion

262 SD OCT has revolutionised the diagnostic and prognostic capabilities for a number of
263 ophthalmic conditions, including diabetic macular oedema, glaucoma, age-related macular
264 degeneration and compressive optic neuropathy.[9,10] Normative databases provide the
265 reference values against which to compare cases of disease states. Although several studies
266 report the normative data for SD OCT,[11–13] to the author’s knowledge, no data exist for
267 SD OCT that includes both macular GCL and peripapillary RNFL scans at the A-scan level.
268 The A-scan is a single point of interrogation on the retina that represents the most basic unit
269 of measurement data in the OCT. Equivalent A-scans represent the same anatomical location
270 across patients. The comparison of A-scan measurements between patients is a more precise
271 analysis than the standard ETDRS grid, which is based on averaged A-scan values across the
272 segments. In the advent of analytical methodologies, such as artificial intelligence and
273 machine learning, it is becoming increasingly possible to use larger volumes of data. The
274 primary purpose of reporting normative A-scans is to facilitate further research into patterns
275 of disease development at the retina beyond the confines of standardised grids, such as
276 ETDRS, using such methodologies.

277 In the creation of a normative database, inclusion and exclusion criteria must be carefully
278 considered to realistically represent the distribution of normal and diseased populations of
279 interest. This study aimed to create a normative dataset of OCT scans for ongoing research of
280 glaucoma and compressive optic neuropathies within the metropolitan region of Melbourne,
281 Australia. An ethnically diverse population was used to represent the target population. All
282 nine of the broad ethnic groups present in Australia were represented in our study population
283 in similar proportions.

284 Five groups showed no statistical difference compared to the known proportions in
285 Melbourne. Given the small sample size and large number of ethnic groups, the database was
286 representative of the target population. The ethnic groups used in this study were extracted
287 from population census data that were designed according to political and geographical
288 boundaries. This may have caused the grouping of some participants with differing genetic
289 influences on their retinal structure. For example, the Americas ethnic group included both
290 African American and Caucasian American people that have been shown to have different
291 OCT measurements.[14,15] This was an unavoidable limitation set by the Australian census
292 groups.[16]

293 This study found a negative association between age and macular thickness, which has been
294 previously demonstrated. All the sectors of the ETDRS grid have been reported to be
295 negatively associated with increasing age, except for the central 1 mm of the retina.[12,17–
296 19] This study is consistent with these findings; however, the negative correlation found in
297 the temporal inner and inferior inner segments was found not to be statistically significant.
298 Similar to other studies, the central area had almost no association ($r = 0.00899$, $p = 0.9008$).
299 This study identified that the GCL and IPL thickness and volume for all the sectors
300 (excluding the centre for the IPL) decreased with age. This was in keeping with findings from

301 previous studies.[12,17] This finding represents a normal process of ageing with loss of
302 RNFLs over time, which has been reported to be between 0.3% and 0.6% of neurons lost per
303 year.[20] This is important for differentiating losses due to age-related processes from those
304 caused by disease processes, such as glaucoma or compressive optic neuropathy.

305 A statistically significant positive correlation was found between increasing age and temporal
306 inner RNFL thickness ($r = 0.1929$, $p = 0.0062$). Similarly, Nieves-Moreno et al. found a
307 positive correlation between temporal inner RNFL and age ($r = 0.256$, $p = <0.001$).¹¹ No
308 other significant correlations were found between RNFL volume or thickness and age in this
309 study. Given that the temporal inner is the thinnest RNFL sector, this study postulated that it
310 would be proportionally the most affected by an increasing thickness observed in the internal
311 limiting membrane with age and, therefore, correlate positively with age. Males were found
312 to have a significantly higher RT, RNFL, GCL and IPL thickness than females. This was
313 most evident in the inner layers, which is similar to the OCT results reported in other
314 studies.[12,17]

315 The Limitations of this study include its retrospective design, which led to missing variables
316 that may have affected the OCT measurements, including the axial length and refraction. This
317 study provides normal baseline data for the comparison of various macular diseases. These
318 data will also be used to monitor patients with glaucoma and compressive optic neuropathy at
319 The RMH.

320 **Acknowledgements**

321 Amanda Rebbechi – medial photographer; Joss Dimock – medical photographer, Debbie
322 Curran – medical photographer;

323 **References**

324

325 1. Huang D, Swanson E, Lin C, Schuman J, Stinson W, Chang W, et al. Optical coherence
326 tomography. *Science*. 1991;254(5035):1178–81.

327 2. Danesh-Meyer HV, Yap J, Frampton C, Savino PJ. Differentiation of Compressive from
328 Glaucomatous Optic Neuropathy with Spectral-Domain Optical Coherence Tomography.
329 *Ophthalmology*. 2014;121(8):1516–23.

330 3. Huang D, Swanson E, Lin C, Schuman J, Stinson W, Chang W, et al. Optical coherence
331 tomography. *Science*. 1991;254(5035):1178–81.

332 4. Group ETDRSR. Grading Diabetic Retinopathy from Stereoscopic Color Fundus
333 Photographs—An Extension of the Modified Airlie House Classification. *Ophthalmology*.
334 1991;98(5):786–806.

335 5. Early photocoagulation for diabetic retinopathy. ETDRS report number 9. Early Treatment
336 Diabetic Retinopathy Study Research Group. *Ophthalmology*. 1991;98(5 Suppl):766–85.

337 6. (ABS) AB of S. Australian Standard Classification of Cultural and Ethnic Groups
338 (ASCCEG) [Internet]. n.d. Available from:
339 <https://www.abs.gov.au/ausstats/abs@.nsf/Previousproducts/1249.0Main%20Features12011?>

340 7. R Development Core Team: A Language and Environment for Statistical Computing.
341 Vienna, Austria: R Foundation for Statistical Computing; 2011.

342 8. Wickham H. *ggplot2: Elegant Graphics for Data Analysis* [Internet]. Springer-Verlag New
343 York; 2016. Available from: <https://ggplot2.tidyverse.org>

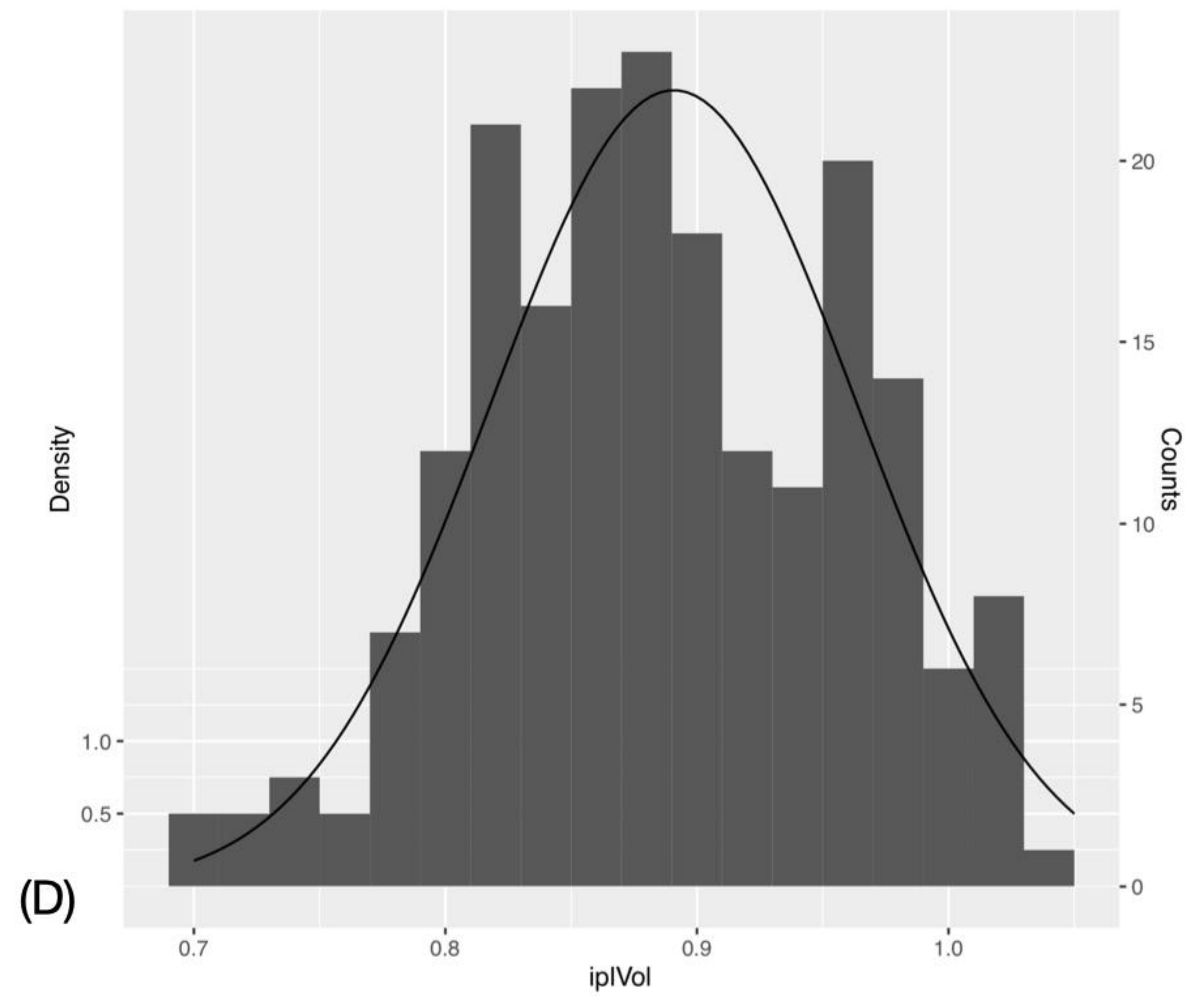
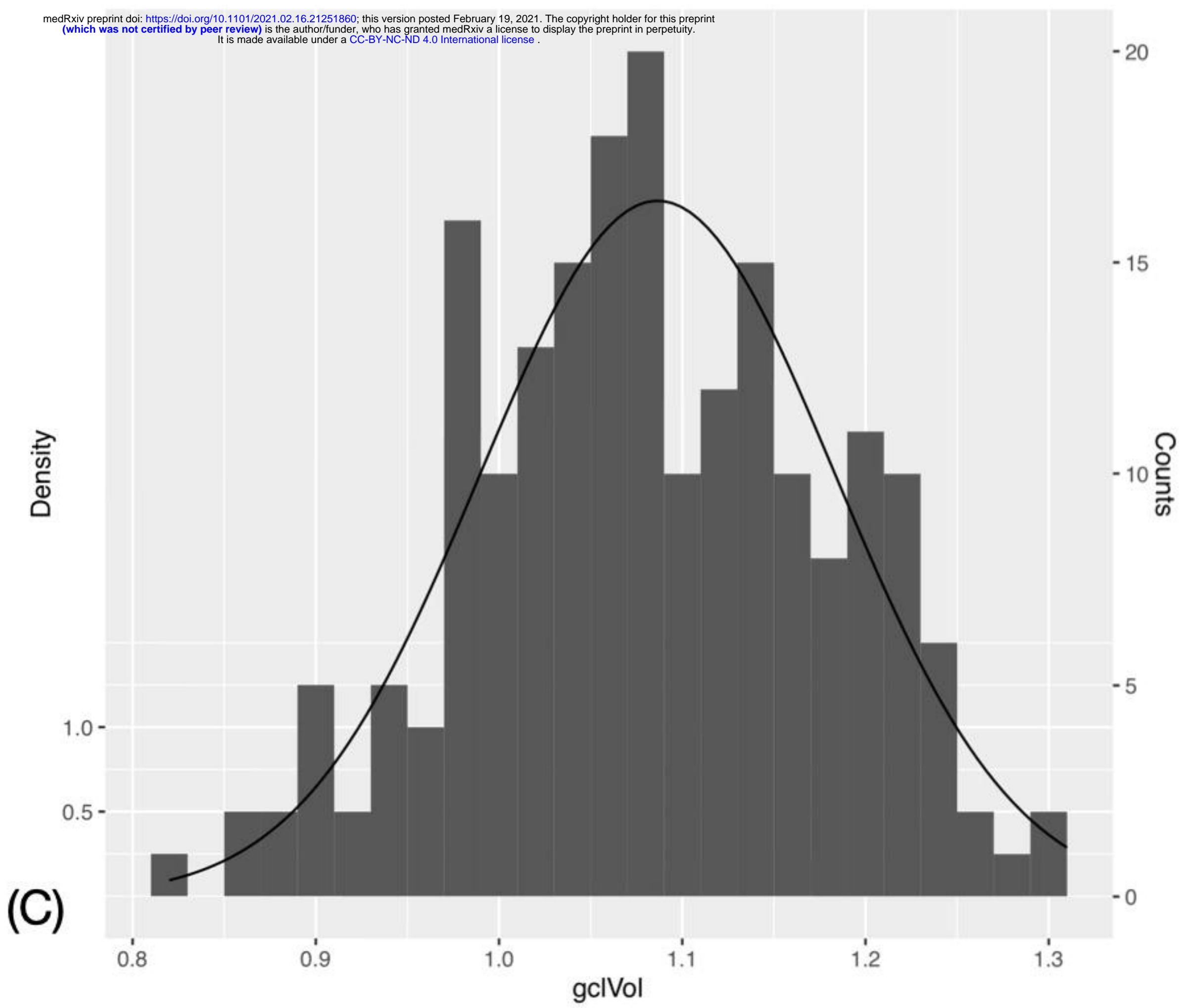
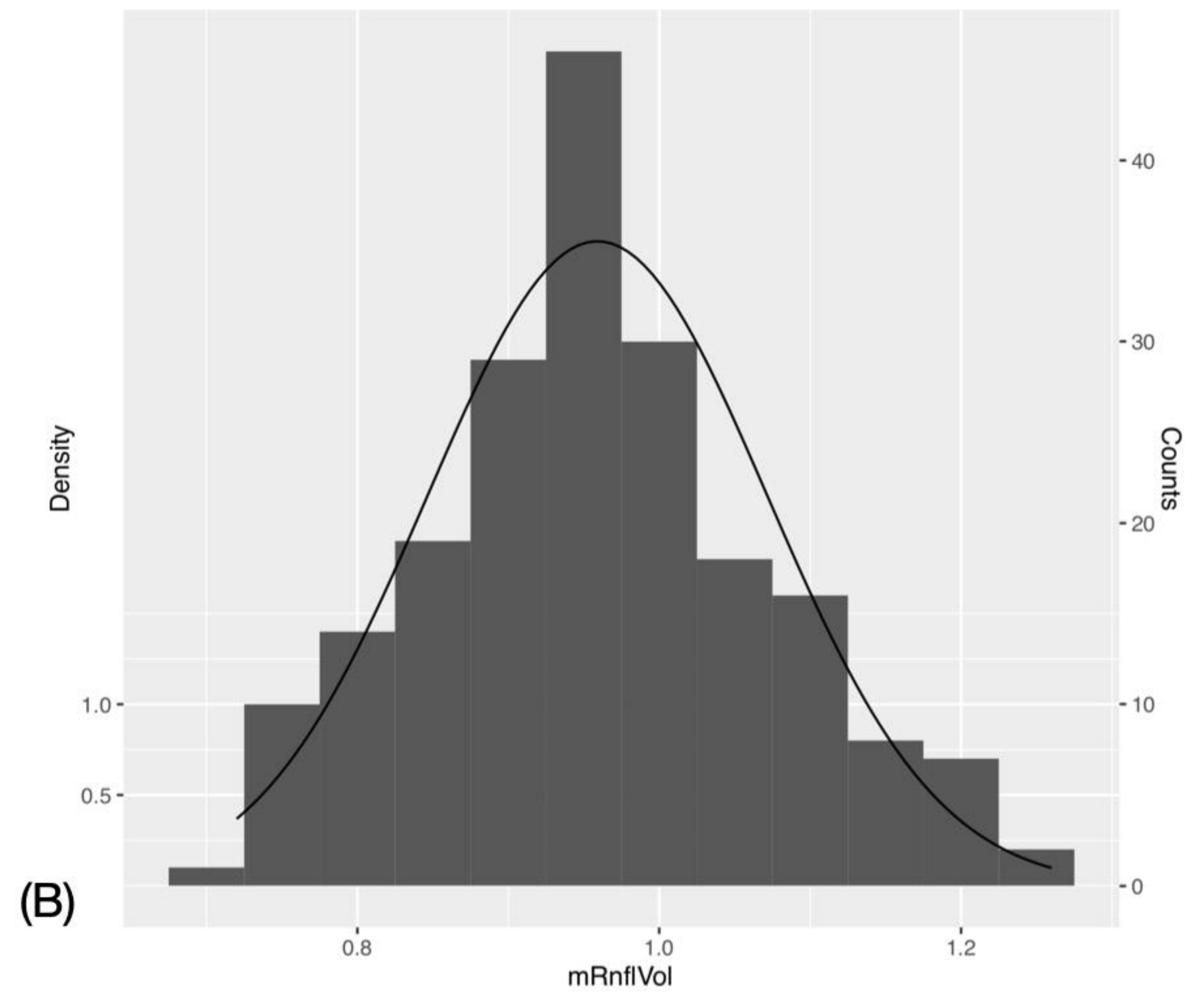
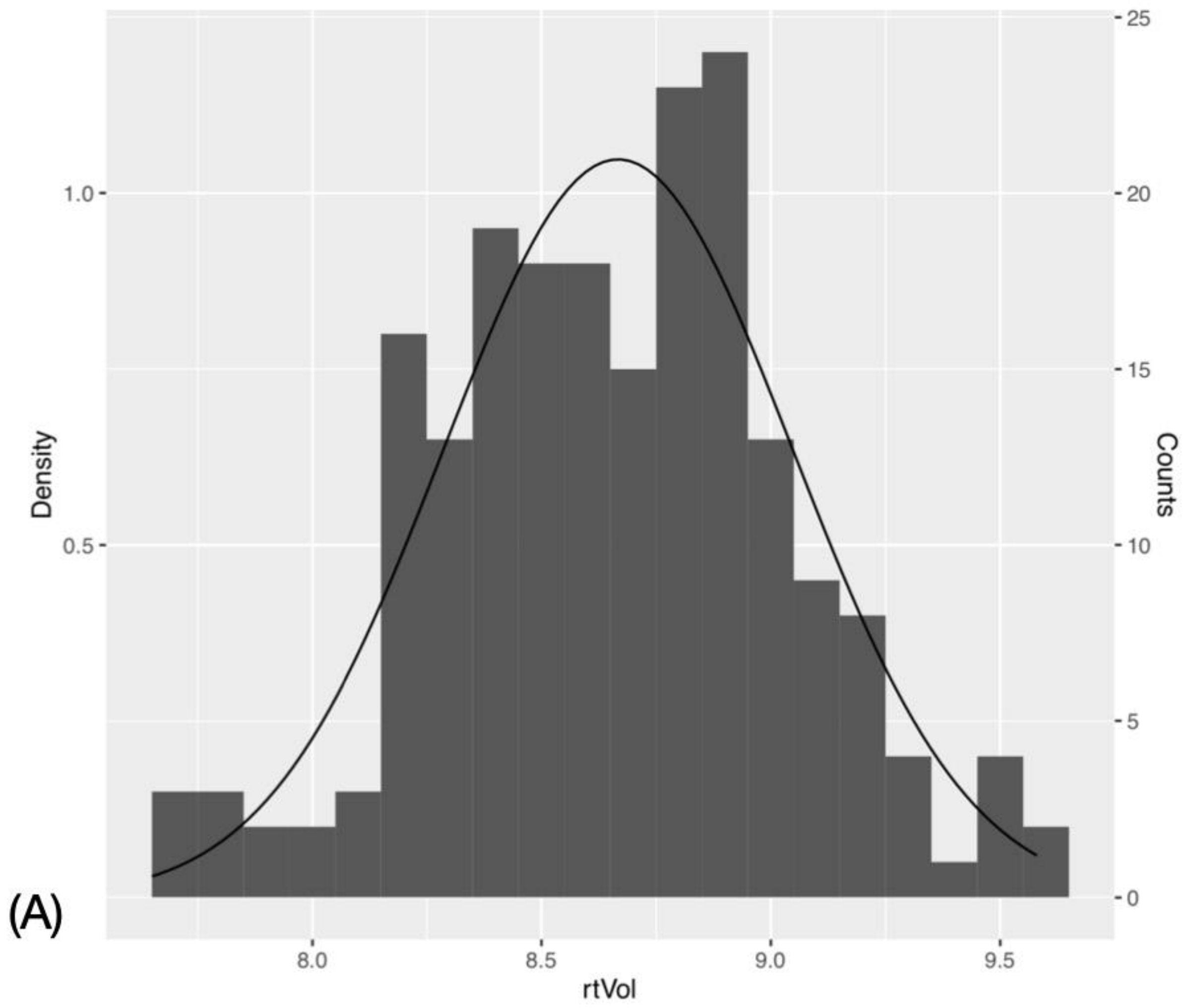
344 9. Danesh-Meyer HV, Wong A, Papchenko T, Matheos K, Stylli S, Nichols A, et al. Optical
345 coherence tomography predicts visual outcome for pituitary tumors. *J Clin Neurosci*.
346 2015;22(7):1098–104.

347 10. Adhi M, Duker JS. Optical coherence tomography--current and future applications. *Curr*
348 *Opin Ophthalmol*. 2013;24(3):213–21.

349 11. Grover S, Murthy RK, Brar VS, Chalam KV. Normative Data for Macular Thickness by
350 High-Definition Spectral-Domain Optical Coherence Tomography (Spectralis). *Am J*
351 *Ophthalmol*. 2009;148(2):266–71.

352 12. Nieves-Moreno M, Martínez-de-la-Casa JM, Cifuentes-Canorea P, Sastre-Ibáñez M,
353 Santos-Bueso E, Sáenz-Francés F, et al. Normative database for separate inner retinal layers

- 354 thickness using spectral domain optical coherence tomography in Caucasian population. *Plos*
355 *One*. 2017;12(7):e0180450.
- 356 13. Appukuttan B, Giridhar A, Gopalakrishnan M, Sivaprasad S. Normative spectral domain
357 optical coherence tomography data on macular and retinal nerve fiber layer thickness in
358 Indians. *Indian J Ophthalmol*. 2014;62(3):316–21.
- 359 14. Kelty PJ, Payne JF, Trivedi RH, Kelty J, Bowie EM, Burger BM. Macular Thickness
360 Assessment in Healthy Eyes Based on Ethnicity Using Stratus OCT Optical Coherence
361 Tomography. *Investigative Ophthalmology Vis Sci*. 2008;49(6):2668.
- 362 15. Kashani AH, Zimmer-Galler IE, Shah SM, Dustin L, Do DV, Elliott D, et al. Retinal
363 Thickness Analysis by Race, Gender, and Age Using Stratus OCT. *Am J Ophthalmol*.
364 2010;149(3):496-502.e1.
- 365 16. Realini T, Zangwill LM, Flanagan JG, Garway-Heath D, Patella VM, Johnson CA, et al.
366 Normative Databases for Imaging Instrumentation. *J Glaucoma*. 2015;24(6):480–3.
- 367 17. Demirkaya N, Dijk HW van, Schuppen SM van, Abràmoff MD, Garvin MK, Sonka M, et
368 al. Effect of Age on Individual Retinal Layer Thickness in Normal Eyes as Measured With
369 Spectral-Domain Optical Coherence Tomography. *Investigative Ophthalmology Vis Sci*.
370 2013;54(7):4934.
- 371 18. Manassakorn A, Chaidaroon W, Ausayakhun S, Aupapong S, Wattananikorn S.
372 Normative database of retinal nerve fiber layer and macular retinal thickness in a Thai
373 population. *Jpn J Ophthalmol*. 2008;52(6):450–6.
- 374 19. Appukuttan B, Giridhar A, Gopalakrishnan M, Sivaprasad S. Normative spectral domain
375 optical coherence tomography data on macular and retinal nerve fiber layer thickness in
376 Indians. *Indian J Ophthalmol*. 2014;62(3):316–21.
- 377 20. Repka MX, Quigley HA. The Effect of Age on Normal Human Optic Nerve Fiver
378 Number and Diameter. *Ophthalmology*. 1989;96(1):26–32.
- 379



Density

Counts

medRxiv preprint doi: <https://doi.org/10.1101/2021.02.16.21251860>; this version posted February 19, 2021. The copyright holder for this preprint (which was not certified by peer review) is the author/funder, who has granted medRxiv a license to display the preprint in perpetuity. It is made available under a [CC-BY-NC-ND 4.0 International license](https://creativecommons.org/licenses/by-nc-nd/4.0/).

